Journal of Applied Polymer Science

Optimal designing of polyurethane-based nanocomposite system for aerostat envelope

U. Chatterjee, B. S. Butola, M. Joshi
Department of Textile Technology, I.I.T, Delhi 110 016, India
Correspondence to: M. Joshi (E-mail: mangala@textile.iitd.ac.in or mangalajoshi9@gmail.com)

ABSTRACT: This article reports an optimal designing of thermoplastic polyurethane (TPU) nanocomposite formulation, particularly targeting aerostat envelope for enhanced weathering and gas barrier properties. The synergistic effect of conventional UV protective additive with advanced nano materials (i.e. nanoclay and graphene) on TPU-based formulations was explored. A series of formulations were prepared in accordance with a mixture design for three components additives (UV stabilizer, nanoclay, and graphene) and coated on to a woven polyester (PET) fabric. The coated systems were evaluated for resistance to UV radiation, resistance to helium gas permeability, and loss in both the properties against accelerated artificial weathering. The composition of the additive mixture was simultaneously optimized by desirability function approach with a view to maximize UV radiation protection and minimize helium gas permeability. © 2016 Wiley Periodicals, Inc. J. Appl. Polym. Sci. **2016**, *133*, 43529.

KEYWORDS: ageing; coatings; composites; nanostructured polymers; polyurethanes

Received 4 November 2015; accepted 9 February 2016
DOI: 10.1002/app.43529

INTRODUCTION

Tethered helium aerostats are receiving renewed attention in the scientific communities. "Aerostat" is an advanced inflatable aerial delivery system having a shape of an aircraft that floats about 3000 ft above from the sea-level for aerial surveillance. These aerostats are used as raised platforms for various electronic payloads ranging from sophisticated airborne early warning radar systems to very low frequency (VLF)/low frequency (LF) communications, active or passive electronic warfare equipment, public emergency broadcasting systems, communications relay, etc. and thus the structures are needed to be exposed in the harsh atmospheric weather for prolonged time. Unlike fixed-wing aircraft or helicopters, aerostats are "lighter-than-air (LTA)", typically use helium gas to stay aloft and are tethered using a mooring system operated from a fixed location. Any damage on the aerostat envelope that affects the barrier property and gives an escape to the helium gas causes an immediate failure of the whole structure leading to loss of crores. From the manufacturing point of view, designing of new and improved materials for this kind of structure that consistently survive in the harsh atmospheric condition is one of the critical issues. A typical inflatable aerostat structure consists of a strength layer generally made up of woven textiles, with high strength-to-weight-ratios, to provide a flexible high strength base to the structure and a protective layer which acts as a gas barrier layer for maintaining the inflated condition of the structure for prolonged time. In such cases, the lifetime of the ultimate inflatable structure is primarily determined by the protective properties of the polymeric layer. Use of conventional polymers (polyvinyl chloride, acrylic, etc.) in these applications gets very limited because of the poor weathering resistance, low flex fatigue, poor adhesion to substrate, or high permeability to air or gases. As an alternative material for the protective layer of the aerostat envelope, thermoplastic polyurethane (TPU) has recently attracted a lot of interest.[1–3] However, similar to other polymer materials, exposure of TPU to aggressive environments (mainly to UV radiation) for prolonged time causes changes in its physical, chemical, and mechanical characteristics and even loss of use value.[4–7] Conventionally, UV stabilizers such as UV absorbers, HALS, antioxidants, etc. are incorporated into the formulation to reduce degradation. But the conventional additives suffer from high physical loss through migration, leaching, blooming, etc. In this regard, incorporation of nanomaterials can be a novel approach. Not only nanomaterials seem to provide minimum physical loss but they can provide additional functional properties also such as resistance to UV radiation, resistance to permeability of gases, etc.

In this respect, the most common nanofiller to improve the impermeability property of polymeric membranes is nanoclay. Nanoclays, having layered structures with large aspect ratios, present a tortuous path for the gas/vapor molecule and thereby

© 2016 Wiley Periodicals, Inc.

Table I. Details of the TPU Resin

Supplier	Bayer Material Science, U.S.A
Type	Aliphatic isocyanates and polyether polyol
Specific gravity	1.08
Glass transition temperature (Tg)	−40 °C
Softening temperature	109 °C
Tensile strength	28.3 MPa
Ultimate elonglation	370%

retard its rate of passage through the polymer matrix.[8,9] Graphene, the exfoliated carbon sheet, has also been reported recently to act as diffusion barriers in polymeric membranes.[10–12] Because of its two-dimensional platelet geometry, graphene also contributes in reducing the permeability. However, developing an effective polymeric system for high weathering performance properties is a complex task. Several variables, such as type and number of additives, their concentration levels in the polymer matrix, the processing of the each additives as well as the processing of the overall formulation, all play a significant role in determining the ultimate properties of the system.

In such cases of multivariate systems, changing of dependable variables at a time and to study their effect on the performance property or response is a complicated labour intensive technique. Design of experiments (DOE) is a statistical technique for optimizing such multivariable systems. Using DOE based on response surface methodology, optimum condition has been achieved in various fields of research with a minimum number of experiments without the need for studying all possible combinations experimentally.[13–19] For experiments that focus specially on formulation or composition, the use of mixture design can be useful.[20–22] However, very few researches have been explored and documented on this methodology, specifically in polymeric field. In a mixture DOE, the independent factors are considered as the proportions of different components for all ingredients of a mixture.

In this work, a three-component mixture design, with an upper bound constraint for one component, was adopted to prepare a series of TPU-based nanocomposite formulations. PET fabric was coated using those formulations and tested for weathering performance. The results of experiments were analyzed statistically by response surface methodology. A set of response surface equations was obtained for predicting the UV protection factor (UPF) as a measure of UV transmittance, helium gas permeability, and loss in both the properties with weathering as a function of composition of mixture used in the formulation. Simultaneous optimization of the four responses was carried out based on desirability function approach.

For the first time, to the authors' knowledge, an optimal design of TPU-based nanocomposite formulation has been proposed to achieve enhanced weathering performance particularly targeting aerostat envelope system.

Table II. Details of Additives

Additives	Specifications
UV protective additive: Tinuvin B75, (BASF, India)	Liquid mixture of 40% UVA+ 40% HALS+ 20% AO
Nanoclay: Cloisite 30B, (Sigma Aldrich, UK)	Organomodified; ballmilled at 400 rpm for 2 h
Graphene: Graphene/DMF dispersion, (United Nanotech Innovations, India)	Predispersed graphene in DMF (3% w/v)

EXPERIMENTAL

Materials

Commercial TPU chips, having aliphatic isocyanate and ether-based polyols (with no free isocyanate present), were procured from Bayer Material Science, U.S.A. Polymer solution was prepared by dissolving the required amount of TPU into Dimethylformamide (DMF) solvent (Merck, India). A commercial UV stabilizer and two different nanomaterials were incorporated later into the slurry as additives. The details of the TPU resin and the additives have been given in Tables I and II, respectively. Plain woven PET fabric of 180 gsm (average breaking load 2950 N/50 mm width, extension at break 32%, as per ISO 7016-2 standard[23] method), as a coating substrate or base, was procured from Kusumgar Corporate, India.

Formulation Design and Preparation of Coated Fabric

A series of TPU nanocomposite coating formulation was planned in accordance with a mixture design for three components (Tinuvin B75, nanoclay, and graphene) with an upper bound constraint for one component (Tinuvin B75 $\leq$ 1.5 wt %). The range of the amount of the additives to be incorporated and their coded forms in the mixture design have been given in Table III. In this work, the effect of nano additives was studied up to 5 wt % concentration as beyond that deterioration in the properties is expected. While, in case of Tinuvin B75 (UV stabilizer) the maximum concentration was reduced to 1.5 wt % for the same reason. In all the formulations, overall 5 wt % additive mixture on the wt. of TPU was incorporated so that in each case the ratio of TPU and additive mixture remain constant. The layout of the design has been shown in Figure 1. As can be seen from the figure, the constraint region forms a trapezoidal shape having over all nine runs (see Table IV) consisting of four vertices, four centers of edges and one centroid. The run points have been chosen

Table III. Specifications of Mixture Design

		Coded value	
Mixture components	Use range (wt %, o.w.f. of TPU)	Low	High
Tinuvin B75	0–1.5%	0	0.3
Nano clay	0–5%	0	1
Graphene	0–5%	0	1

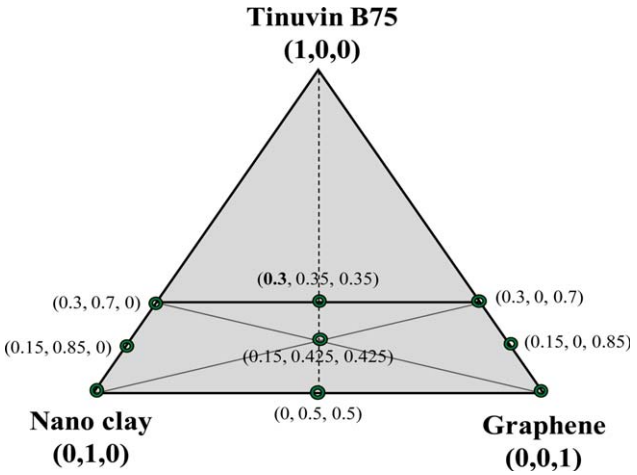

Figure 1. Layout of the mixture design with an upper bound constraint for one component (values in the bracket define the weight proportion of each component at that specific point). [Color figure can be viewed in the online issue, which is available at wileyonlinelibrary.com.]

using Design-Expert® software and each run point defines a formulation consisting of the weight proportions of the three components that sums to 1.

TPU chips were first dried at 80 °C for 3 h under vacuum oven to remove any moisture content. Measured amount of dried polyurethane chips (10 wt %) were overnight kept in DMF for swelling. The mixture was then heated gradually up to 50 °C for 3 h in water bath and then magnetically stirred for another 3 h at 50 °C to get clear solution. Required amount of Tinuvin B 75 was first dissolved into DMF and then directly added to the TPU solution. Clay (dried at 90 °C for 6 h and ball-milled at 200 rpm for 2 h)[24] and graphene were also dispersed into DMF first using ultrasonication for few minutes and then mixed into the TPU solution with high speed magnetic stirring. The TPU nanocomposite formulation was coated on to plain woven PET base fabric by a continuous solution coating machine (Mathis, Switzerland; Model: KTF-S) using knife over roll coating method. The solvent was evaporated by hot air (140 °C temperature and 2000 rpm fan speed) into the drying chamber of the machine. In the whole process of coating the web run was maintained as low as 0.3 mt/min for complete evaporation of the solvent. The solid content of the coating after drying was kept at a level of 100 g/m^2 of fabric. So, as per the design planned, total nine types of coated fabrics were prepared separately for evaluation.

Testing of the Coated Fabric

Four response values for each coated fabric were tested as the measure of weathering performance and the results were analyzed by using Design-Expert® software version 9. UPF values as a gauge of UV transmittance of the prepared coated fabric were measured by UV transmittance analyzer, Labsphere 2000F following AATCC 183 standard.[25] Helium gas permeability through the coated fabrics has been measured by the in-house developed gas permeability tester following ASTM D-1434-82 standard[26] at an initial pressure of 20 cm water column height and 25 °C average temperature. The amount of gas permeating through the sample was recorded from the manometer displacement after 24 h. All the samples were weathered in accelerated weatherometer (Xenotest Beta+, ATLAS) for 100 h following ISO 4892 method[27] (refer Table V) and then the loss in both UPF and gas permeability of the coated fabrics were measured and calculated in percentage value. A scanning electron microscope (ZEISS, EVO50) was used to observe the surface morphology of coated fabrics.

Simultaneous Optimization

The desirability function approach was adopted to optimize the four responses simultaneously. This approach was introduced by Harrington[28] and developed further by Derringer and Suich.[29] The desirability function is based on the search for a global optimum $[Ds = f(Y_i)]$ by the transformation of the measured properties or the responses (Y_i) to a dimensionless scale for each criterion.

In the optimization, each response (Y_i) is associated with its own partial desirability function (ds_i) that varies from 0 (for completely undesirable) to 1 (for most desirable) according to the closeness of the response to its target value. If the response is of the "target is best" kind, then the partial desirability is defined in the following equation:

$$ds_i = \begin{cases} 0, & \text{if } Y_i < Lv_i \\ \left|\frac{Y_i - Lv_i}{Tv_i - Lv_i}\right|^{sv}, & \text{if } Lv_i \le Y_i \le Tv_i \\ \left|\frac{Y_i - Uv_i}{Tv_i - Uv_i}\right|^{tv}, & \text{if } Tv_i \le Y_i \le Uv_i \\ 0, & \text{if } Y_i > Uv_i \end{cases} \quad (1)$$

where Y_i represents the predicted response, Lv_i, Uv_i, and Tv_i denote the lower, upper, and target values, respectively, that are desired for response Y_i, with $Lv_i \le Tv_i \le Uv_i$, and sv and tv indicate the importance of achieving the target value. For $sv = tv = 1$, the desirability function increases linearly towards Tv_i; for $sv < 1$ and $tv < 1$, the function is convex and for $sv > 1$ and $tv > 1$, the function is concave. If the response is required to be maximized, then the partial desirability is defined in the following equation:

$$ds_i = \begin{cases} 0, & \text{if } Y_i < Lv_i \\ \left|\frac{Y_i - Lv_i}{Tv_i - Lv_i}\right|^{sv}, & \text{if } Lv_i \le Y_i \le Tv_i \\ 1, & \text{if } Y_i > Tv_i \end{cases} \quad (2)$$

If the response is required to be minimized, then the partial desirability is defined in the following equation:

$$ds_i = \begin{cases} 1, & \text{if } Y_i < Tv_i \\ \left|\frac{Y_i - Uv_i}{Tv_i - Uv_i}\right|^{sv}, & \text{if } Tv_i \le Y_i \le Uv_i \\ 0, & , \text{if } Y_i > Uv_i \end{cases} \quad (3)$$

The individual desirability functions for all the responses are then combined, as the geometric mean, to obtain the global desirability function (D_s), as defined in the following equation:

Table IV. TPU Nanocomposite Compositions and Performance Properties of Coated Fabrics

	Weight proportion of additive components			Response 1	Response 2	Response 3	Response 4
Run	A: Tinuvin B 75	B: Nano clay	C: Graphene	UPF	UPF loss %	Gas barrier Lt/m^2/day	Gas barrier loss %
1	0.000	1.000	0.000	99.20	18.64	2.29	3.41
2	0.000	0.000	1.000	113.90	15.63	0.50	4.57
3	0.300	0.700	0.000	327.82	13.60	0.68	19.55
4	0.300	0.000	0.700	351.43	21.19	0.15	19.46
5	0.000	0.500	0.500	115.09	10.92	0.91	6.88
6	0.150	0.850	0.000	202.91	14.41	1.91	10.92
7	0.150	0.000	0.850	297.98	17.50	1.02	11.00
8	0.300	0.350	0.350	325.12	15.31	0.29	20.69
9	0.150	0.425	0.425	251.57	10.53	0.90	12.06

$$Ds=\left(\prod_{i=1}^{i=p} ds_i^{w_i}\right)^{\frac{1}{p}} \quad (4)$$

where w_i denotes the relative importance assigned to the ith response and p is total number of responses. Finally, the maximum value of the global desirability function (D_s) can be obtained from the above analysis.

RESULTS AND DISCUSSION

UPF Values

The UPF values of the nine fabric coated with different compositions of TPU nanocomposite have been reported in Table IV. For run 4, with additive composition Tinuvin B75 = 0.30 (weight proportion) and graphene = 0.70 exhibited the highest UPF value; whereas for run 1, with nanoclay = 1.00 registered the lowest UPF value (refer Table IV). This is very obvious that formulation with highest Tinuvin B75 will exhibit highest UPF value as Tinuvion B75 is a commercial UV stabilizer having property to directly absorb UV light energy. Graphene, being composed of carbon sheet, can enhance the UPF value by absorbing UV radiation. Nanoclay exhibited least contribution in absorbing UV radiation compared to the other two additives.

Table V. Details of Accelerated Artificial Weathering Test Program

Parameters	Specifications
Type of lamp	Xenon arc
Type of filters	Inner filter glass—Type "S" Borosilicate Outer filter glass—Type "S" Borosilicate
Total irradiance	60 watt/m^2 (300–400 nm)
Dry-wet cycle	Exposure of 1 h 42 min in xenon arc 18 min exposure to xenon arc with water spray
Black panel temperature	65 ± 3 °C
Relative humidity	50 ± 5%
Duration of exposure	100 h

The experimental data of UPF values were fitted to a linear model and the following expression [eq. (5)] was obtained where A, B, and C denote the weight proportion (dimensionless) of Tinuvin B 75, nanoclay, and graphene, respectively.

$$UPF=853.62A+94.69B+154.37C \quad (5)$$

The equation was fitted in the Design-Expert® software using regression technique. The results of analysis of variance of the aforesaid model of UPF are reported in Table VI(a). It can be seen that the model was highly significant at a very small level of significance (P value < 0.0001). The coefficient of determination (R^2) between the predicted and measured UPF values was found as 0.9632. Figure 2 plots the contours of UPF values along with the design points shown by solid circles. It can be seen from the equation that, if maximum UPF is desired alone, a pure mixture of Tinuvin B75 need to be chosen.

Loss in UPF

The percentage loss in UPF value of the coated fabrics after 100 h weathering has been reported in Table IV. Minimum loss was found with the formulation consisting 0.50 nanoclay and 0.50 graphene and no Tinuvin B75 (run 5). Run 4, with maximum amount of Tinuvin B75 (0.30) and graphene (0.70), offered the maximum loss in the UPF value. This is an indicative fact that, although Tinuvin B75 is giving maximum UPF value, however, it is providing maximum loss in UPF value also. This is because of the high physical loss of Tinuvin B75 through migration, blooming, evaporation, or leaching which is the main problem related to this kind of commercially available UV stabilizers. In the Design-Expert® software, the experimental data of the percentage loss in the UPF (UPF_L) values was well fitted to a quadratic model by regression technique and the following expression [eq. (6)] was obtained:

$$UPF_L=74.53A+18.71B+15.64C-102.26AB-56.29AC-25.33BC \quad (6)$$

It can be observed that all the individual effects (A, B, C) as well as the interaction effects (AB, AC, BC) were significant. It was observed that a blending of additives resulted in additional minimization in the loss of UPF as evident from the negative coefficients of the interaction parameters. As it is desirable to

Table VI. Analysis of Variance of Responses

Source	Sum of squares	Degrees of freedom	Mean square	*F*-value	Probability
a. Analysis of variance of UPF					
Model	75,701.84	2	37,850.92	78.52	< 0.0001
Linear Mixture	75,701.84	2	37,850.92	78.52	< 0.0001
Residual	2892.28	6	482.05		
Total	78,594.12	8			
b. Analysis of variance of loss in UP					
Model	95.28	5	19.06	47.84	0.0046
Linear Mixture	9.52	2	4.76	11.95	0.0372
AB	10.42	1	10.42	26.15	0.0145
AC	3.16	1	3.16	7.93	0.0670
BC	47.11	1	47.11	118.28	0.0017
Residual	1.19	3	0.40		
Total	96.48	8			
c. Analysis of variance of helium gas permeability					
Model	4.03	5	0.81	51.38	0.0042
Linear Mixture	3.03	2	1.51	96.58	0.0019
AB	0.36	1	0.36	23.10	0.0171
AC	0.51	1	0.51	32.72	0.0106
BC	0.35	1	0.35	22.16	0.0181
Residual	0.047	3	0.016		
Total	4.08	8			
d. Analysis of variance of loss in helium gas permeability					
Model	345.17	5	69.03	446.06	0.0002
Linear Mixture	335.54	2	167.77	1084.04	< 0.0001
AB	2.08	1	2.08	13.45	0.0351
AC	2.53	1	2.53	16.33	0.0273
BC	6.88	1	6.88	44.45	0.0069
Residual	0.46	3	0.15		
Total	345.64	8			

minimize the loss in UPF value, blending of additives exhibits better results than would have expected just by averaging the loss values of the corresponding pure formulations. The explanation could be the delayed migration of Tinuvin B 75 with time when incorporated into the polymer along with the nano-additives in layered structures.

The results of analysis of variance of the aforesaid model of loss in UPF are reported in Table VI(b). It can be seen that the model was significant at a very small level of significance (P value = 0.0046) and with a R^2 value of 0.8760. Figure 3 plots the contours of loss in UPF.

Helium Gas Permeability

The helium gas permeability values (lt/m^2/day) of the coated fabrics have been reported in Table IV and quite interesting results were found. Minimum permeability value was obtained for run 4 with 0.70 graphene and 0.30 Tinuvin B75, however, the maximum was for 1.00 clay (run 1). As the weight proportion of nanomaterials increased from 0.70 to 0.85 to 1.00, for both nanoclay and graphene, permeability values increased significantly and this may be because of the effect of poor dispersion and agglomeration at higher concentration of nanomaterials.

Values of helium gas permeability (k) were fitted to a quadratic model by regression technique with R^2= 0.9885 and the following equation was found:

$$k = -16.38A + 2.28B + 0.54C + 19.07AB + 22.70AC - 2.17BC \quad (7)$$

The results of analysis of variance of the aforesaid model of helium gas permeability are reported in Table VI(c). It can be seen that the model was significant at a very small level of significance (P value = 0.0042). As the amount of Tinuvin B75 increases, the amount of nanomaterials simultaneously decreases to keep the overall additive concentration constant (5 wt %). At lower concentration, better dispersion of the nanomaterials into the polymer matrix is expected which ultimately decreases the gas permeability value. Figure 4 plots the contours of helium gas permeability.

Loss in Helium Gas Permeability

The percentage loss in helium gas permeability values of the coated fabrics after 100 h weathering has been reported in Table

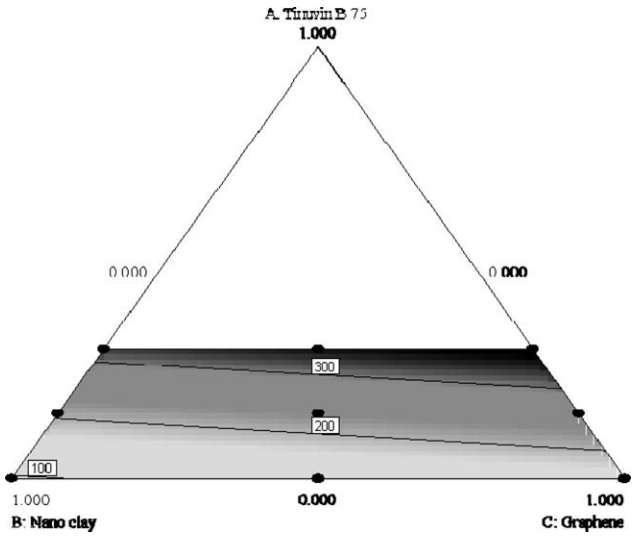

Figure 2. Contour plot of UPF values.

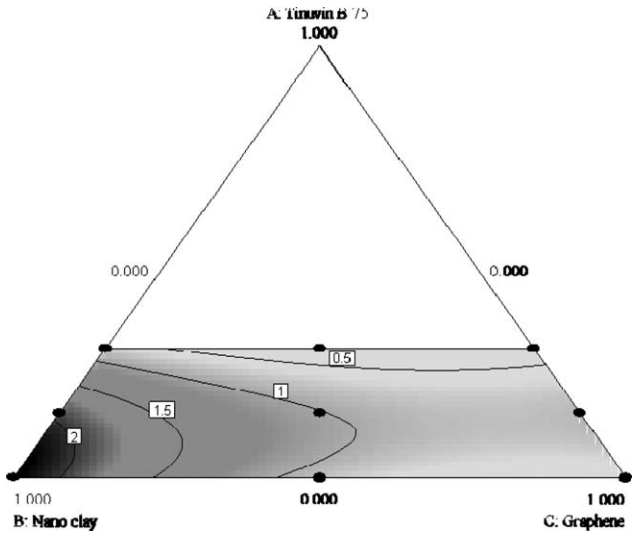

Figure 4. Contour plot of helium gas permeability.

IV. Interestingly, losses were found to be higher where maximum amount of Tinuvin B75 was used, i.e. for run 8, run 3, and run 4 and minimum were for pure clay (run 1), pure graphene (run 2) and even for clay graphene mixture (run 5). This again indicates the physical loss of Tinuvin B75 with weathering.

Although Tinuvin B75 does not directly affect the permeability values but it helps the polymer chain to avoid degradation against weathering which ultimately improves the impermeability property of the coatings with weathering. On the other hand, migration and physical loss of nanomaterials from polymeric materials is truly a difficult task owing to their superior interfacial interaction.[30] Thus the formulations with nanomaterials almost retained the impermeability properties of the coatings. The percentage loss in the He gas permeability (k_L) values were well fitted to a quadratic model again by regression technique ($R^2 = 0.9987$) with the following equation:

$$k_L = 88.98A + 3.61B + 4.68C - 45.71AB - 50.37AC + 9.68BC \quad (8)$$

The results of analysis of variance of the aforesaid model of helium gas permeability are reported in Table VI(d). It can be seen that the model was significant at a very small level of significance (P value = 0.0002). It can also be observed from the equation that Tinuvin B75 along with nanomaterials facilitate in lowering the loss value, thus registering a synergistic influence between the components. Figure 5 plots the contours of loss in helium gas permeability.

Optimization of Responses

Design-Expert® software was used to optimize four responses simultaneously by desirability function approach. UPF value was required to be maximized; however, minimum helium gas permeability was desirable. On the other hand, loss in UPF and loss in helium gas permeability both were required to be minimized. Thus, as stated before (refer Simultaneous Optimization section), the partial desirability functions (ds_i) were calculated following

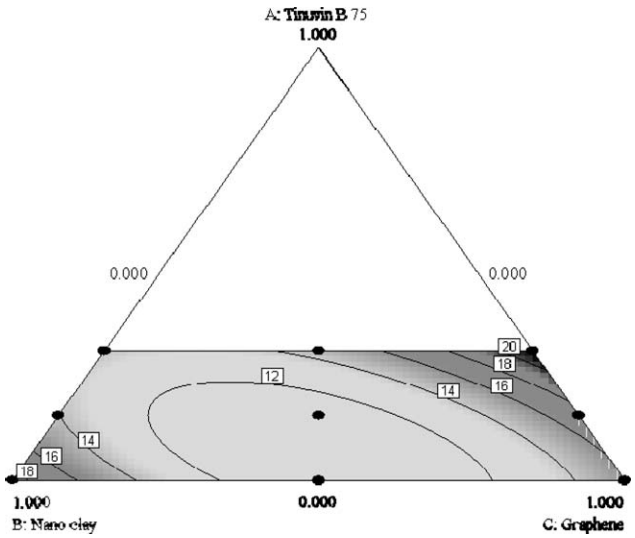

Figure 3. Contour plot of loss in UPF value after weathering.

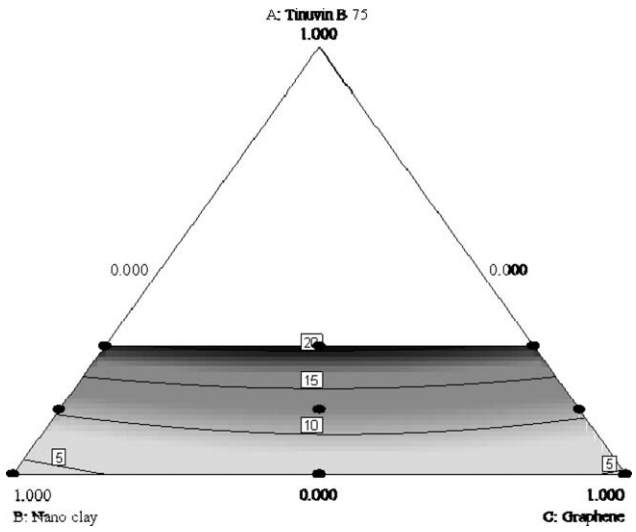

Figure 5. Contour plot of loss in helium gas permeability after weathering.

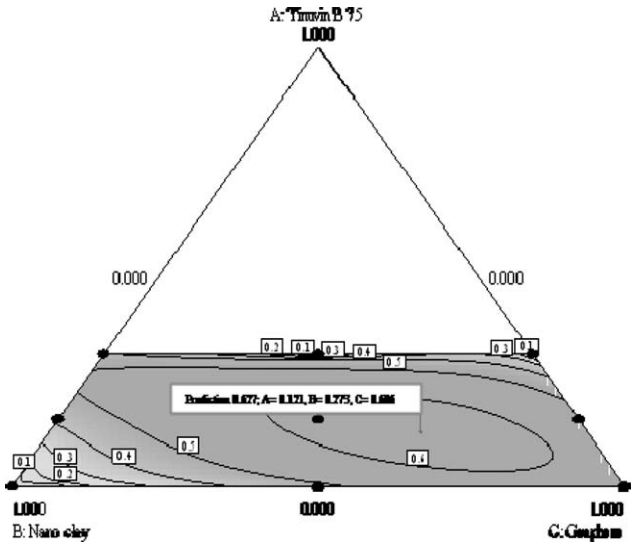

Figure 6. Contour plot of global desirability.

eq. (3) for UPF and eq. (2) for the rest of the responses. Further, all the four responses were considered to be equally important with the highest degree of importance ($w_i = 5$) and finally, the global desirability function (D_s) was calculated following eq. (4). From the behavior of D_s, as displayed in Figure 6, it can be observed that the highest value of D_s is 0.627 where the weight proportion of the coating formulation was predicted as A:B:C = 0.121:0.273:0.606 to get the UPF value 222.55, loss in UPF 11.90%, helium gas permeability 0.90 lt/m^2/day and loss in helium gas permeability 10.97%. So, the predicted values of the optimized formulation are 0.605 wt % Tinuvin B75, 1.365 wt % nanoclay, and 3.030 wt % graphene.

Table VII. Predicted and Actual Values of Responses

Values	UPF	UPF loss (%)	Gas barrier (lt m^{-2} day^{-1})	Gas barrier loss (%)
Predicted	222.55	11.90	0.90	10.97
Actual	234.72	7.50	0.98	7.00

In order to verify this, a TPU nanocomposite-coated fabric was prepared with formulation containing 0.61 wt % Tinuvin B75, 1.36 wt % nano clay, and 3.03 wt % graphene and the UPF value, loss in UPF, helium gas permeability and loss in helium gas permeability were measured as 234.72, 7.5%, 0.98 lt/m^2/day and 7%, respectively (Table VII). The predicted responses from the model were thus found in close agreement with the experimental data. Figures 7(a–c) show the scanning electron microscopic (SEM) images of the base fabric and the coated fabric with the optimized formulation, before and after weathering. No

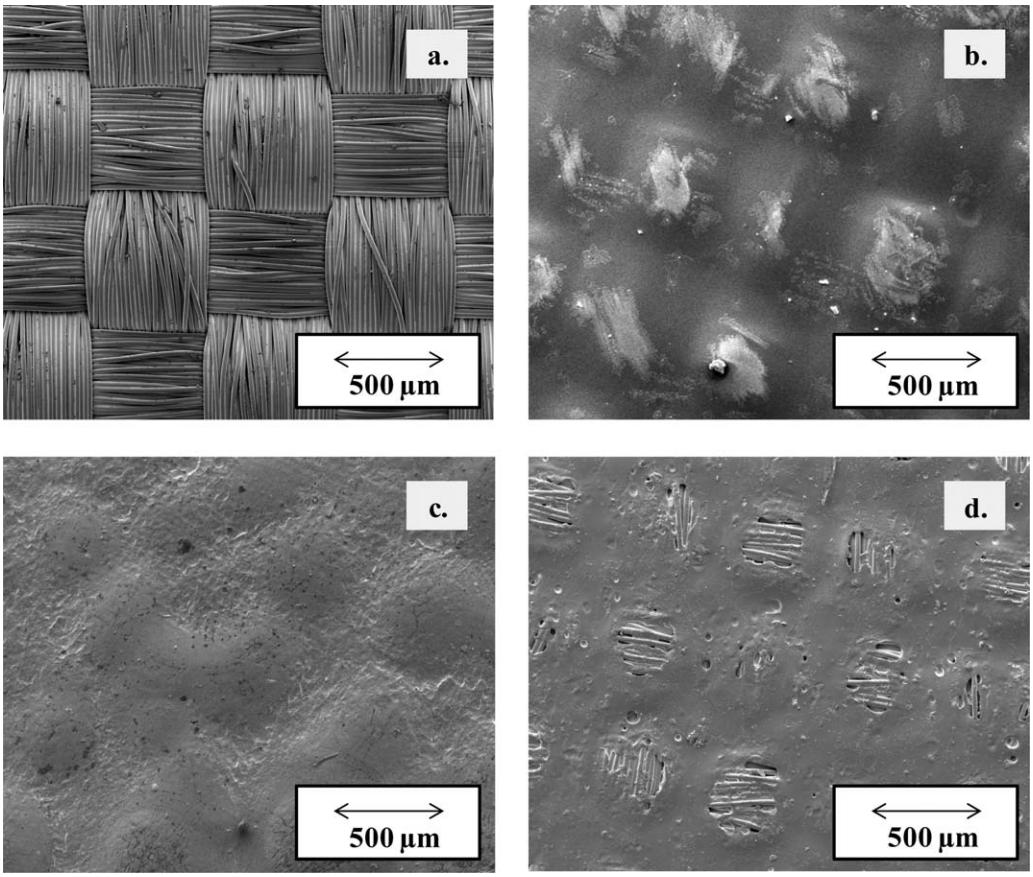

Figure 7. SEM images of (a) base fabric; (b) coated fabric with optimized formulation; (c) coated fabric with optimized formulation and weathered for 100 h; and (d) coated fabric with formulation "run 8" and weathered for 100 h.

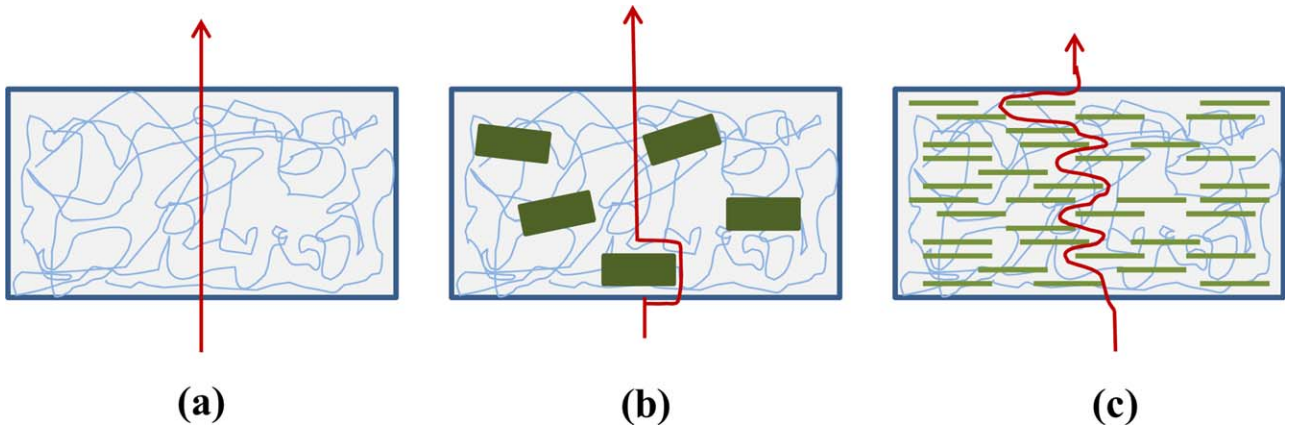

Figure 8. Permeation of gas through the (a) polymer, (b) polymer with micro-additives, and (c) polymer with nano additives. [Color figure can be viewed in the online issue, which is available at wileyonlinelibrary.com.]

significant degradation was found in case of the optimized coated fabric. However, Figure 7(d) (coated fabric with run 8 formulation after weathering) shows small pores and cracks on the surface indicating high degree of degradation which is also evident from the high loss in gas permeability value (see Table IV).

PHYSICAL SIGNIFICANCE

The commercial UV protective additives or stabilizers (such as Tinuvin B 75) function by absorbing incident UV radiation and dispersing the absorbed energy in a nondestructive manner and/or by quenching the free radicals generated with irradiation. Their overall effectiveness in preventing UV degradation of the polymer depends on numerous factors, including absorptivity, compatibility, stability, and distribution within the polymer.[31] Their UV absorption effectiveness is a function of their concentration in the polymer, especially near the surface. This prevents the penetration or transmission of UV radiation through the polymeric coating and thus gives higher UPF value.

However, the inherent chemical efficiency and photostability of UV stabilizers cannot be fully exploited as they suffer from physical losses because of volatility or leaching into the surrounding environment with time.[31,32] Physical loss of the UV absorber involves its removal from the surface by evaporation or dissolution. This loss of the UV stabilizers affects in lowering their concentration in the surface of the polymeric coating and thereby become unavailable to prevent the transmission of UV radiation through the coating which ultimately leads to reduce the UPF value sharply. Thus, the coating consisting of Tinuvin B75 exhibited highest UPF value initially but have shown highest loss in UPF with weathering time.

In comparison, possibility of migration and physical loss of nanoparticles from polymeric materials is a difficult task owing to their superior interfacial interaction and less susceptibility towards evaporation or leaching.[30] Literature also reports lower extent of degradation with time in case of nano material filled polymers than the pristine one.[33,34] Thus, for nanocomposite-based coating, although the UPF value, before weathering, was lower as compared to Tinuvin B 75, but, loss in UPF value with weathering was also found to be significantly lower.

The gas permeation through any polymeric membrane is a diffusion process. In this study, the incorporation of the two-dimensional nanosheets, both the nanoclay and graphene, into the polymer matrix was found to decrease the gas permeability remarkably because of the formation of the tortuous path in the polymer membrane.[8–12,35,36] In a tortuous path, the distances that the diffusing molecules must travel are maximized and this defines the decrease in the permeability as can be seen in Figure 8. The gas passes through a pathway with great difficulty and requires a much longer period of time to permeate. The development of the interface regions between polymer bulk and nano sheets decreases the permeation rate as the filler particles in the membrane is said to be impermeable to the permeant molecules. As compared to microfillers, nanofillers (at same loading) create more tortuous path and are able to enhance the barrier property significantly. However, with a high loading of nanofillers, agglomerations happen and they may act then as microfillers only. Several literatures have reported that nanofillers at higher concentration produce agglomerations and thus the ultimate property of the composite deteriorates.[37–39]

CONCLUSIONS

A series of TPU-based nanocomposite coatings were prepared incorporating ingredients such as UV stabilizer, nanoclay, and graphene and coated on woven PET base particularly targeting aerostat application. The coated systems were evaluated for efficiency to UV resistance, helium gas impermeability and also for the losses in both the properties with weathering. A three-component mixture design in conjunction with the analysis using response surface methodology was employed. A set of expressions were obtained for predicting the evaluated responses as a function of proportion of additive mixtures of the coatings. The additives registered a synergistic effect on the responses. Also, in most of the cases, a binary or ternary blending of additives resulted in desired values of responses than would have expected just by averaging the responses of the corresponding pure blends. The coating consisting of Tinuvin B75 exhibited highest UPF value but highest loss in UPF too. On the other hand, nanoclay and graphene showed little effect in UPF but much better efficiency in retaining the

helium gas impermeability as well as UPF as is evident by much lowered loss in both the properties after exposure to weathering. As a compromise for simultaneously achieving maximum UPF value of 222.55, minimum loss in UPF of 11.90%, minimum helium gas permeability of 0.90 lt/m^2/day and minimum loss in helium gas permeability of 10.97%; the optimum mixture predicted consisting of 0.61 wt % Tinuvin B75, 1.36 wt % nano clay, and 3.03 wt % graphene. It is further confirmed that the predicted responses were in close agreement with the experimental data.

ACKNOWLEDGMENTS

The authors sincerely acknowledge the Aerial Delivery Research and Development Organization (ADRDE), DRDO, India for extending the accelerated weathering facility used in this work and also sponsoring the research project under which this work has been carried out.

REFERENCES

1. Chattopadhyay, D.; Raju, K. *Prog. Polym. Sci.* **2007**, *32*, 352.
2. Mater, C. E. and Kinnel, M. J. (Ilc Dover, Inc.). U.S. Pat. 5,118,558 A, (**1992**).
3. Datta, J.; Laski, M.; Kucinska, J. L. *Przemysł Chemiczny* **2007**, *86*, 63.
4. Boubakri, A.; Guermazi, N.; Elleuch, K.; Ayedi, H. *Mater. Sci. Eng. A* **2010**, *527*, 1649.
5. Beachell, H. C.; Son, C. P. N. *J. Appl. Polym. Sci.* **1964**, *88*, 1089.
6. Aglan, H.; Calhoun, M.; Allie, L. *J. Appl. Polym. Sci.* **2008**, *108*, 558.
7. Rabea, A. M.; Mirabedini, S. M.; Mohseni, M. *J. Appl. Polym. Sci.* **2012**, *124*, 3082.
8. Ray, S. S.; In Clay-Containing Polymer Nanocomposites: From Fundamentals to Real Applications; Ray, S. S., Ed.; Elsevier: Amsterdam, **2013**; Chapter 6, p 227.
9. Choudalakis, G.; Gotsis, A. *Eur. Polym. J.* **2009**, *45*, 967.
10. Kim, H.; Miura, Y.; Macosko, C. W. *Chem. Mater.* **2010**, *22*, 3441.
11. Kalaitzidou, K.; Fukushima, H.; Drzal, L. T. *Carbon* **2007**, *45*, 1446.
12. Kim, H.; Macosko, C. W. *Polymer* **2009**, *50*, 3797.
13. Aslan, N.; Cebeci, Y. *Fuel* **2007**, *86*, 90.
14. Demirel, B.; Daver, F. *J. Appl. Polym. Sci.* **2009**, *114*, 1126.
15. Sharma, S.; Sharma, N.; Gupta, G. D. *Arch. Pharm. Res.* **2010**, *33*, 1199.
16. Banerjee, S.; Joshi, M.; Ghosh, A. K. *J. Appl. Polym. Sci.* **2012**, *123*, 2042.
17. Lee, J.; Nouranian, S.; Torres, G. W.; Lacy, T. E.; Toghiani, H.; Pittman, C. U.; DuBien, J. L. *J. Appl. Polym. Sci.* **2013**, *130*, 2087.
18. Nasef, M. M.; Shamsaei, E.; Ghassemi, P.; Aly, A. A.; Yahaya, A. H. *J. Appl. Polym. Sci.* **2013**, *127*, 1659.
19. Barick, A. K.; Jung, J. Y.; Choi, M. C.; Chang, Y. W. *J. Appl. Polym. Sci.* **2013**, *129*, 1405.
20. Das, D.; Mukhopadhyay, S.; Kaur, H. *J. Compos. Mater.* **2012**, *46*, 3311.
21. Pradhan, A. K.; Das, D.; Chattopadhyay, R.; Singh, S. N. *J. Ind. Text.* **2014**, DOI: 10.1177/1528083714559566.
22. Anderson, M. J.; Whitcomb, P. J.; In Coatings Technnology Handbook; Tracton, A. A., Ed.; CRC Press: U.S., **2005**; Vol. *1*, Chapter 15, p 15-1.
23. IS 7016-2. Methods of Test for Coated and Treated Fabrics Part II: Determination of Breaking Strength and Extension at Break.
24. Stankowski, M.; Kropidłowska, A.; Gazda, M.; Haponiuk, J. T. *J. Therm. Anal. Calorim.* **2008**, *94*, 817.
25. AATCC 183. Transmittance or Blocking of Erythemally Weighted Ultraviolet Radiation through Fabrics.
26. ASTM D-1434-82. Standard Test Method for Determining Gas Permeability Characteristics of Plastic Film and Sheeting.
27. ISO 4892-2. Plastics-Methods of Exposure to Laboratory Light Sources-Part 2: Xenon-arc Lamps.
28. Harrington, E. *J. Ind. Qual. Control* **1956**, *21*, 494.
29. Derringer, G.; Suich, R. *J. Qual. Technol.* **1980**, *44*, 214.
30. Kumar, A. P.; Depan, D.; Tomer, N. S.; Singh, R. P. *Prog. Polym. Sci.* **2009**, *34*, 479.
31. Pickett, J. E. In Service Life Prediction: Methodology and Metrologies; Martin, J. W., Bauer, D. R., Eds.; ACS Publications: New York, **2000**; Vol. *805*, Chapter 12, p 250.
32. Pickett, J. E. *J. Test. Eval* **2004**, *32*, 240.
33. Nuraje, N.; Khan, S. I.; Misak, H.; Asmatulu, R. *ISRN Polym. Sci.* **2013**, *2013*, 1.
34. Wang, H.; Wang, Y.; Liu, D.; Sun, Z.; Wang, H. *J. Nanomater.* **2014**, *2014*, 1.
35. Shamini, G.; Yusoh, K. *Int. J. Chem. Eng. Appl.* **2014**, *5*, 64.
36. Xiao, H.; Ping, Z. H.; Xie, J. W.; Yu, T. Y. *J. Appl. Poly. Sci* **1990**, *40*, 1131.
37. Balasubramanian, M. and Jawahar, P., In Polymer Nanocomposites Based on Inorganic and Organic Nanomaterials; Mohanty, S., Nayak, S. K., Kaith, B. S., Kalia, S., Eds.; Wiley: NJ, **2015**; Vol. *1*, Chapter 9, p 259.
38. Litchfield, D. W.; Baird, D. G. *Polymer* **2008**, *49*, 5027.
39. Modesti, M.; Besco, S.; and Lorenzetti, A. In Optimization of Polymer Nanocomposite Properties; Mittal, V., Ed.; Wiley: Weinheim, **2009**; Vol. *1*, Chapter 17, p 369.